Clinical Trial/Experimental Study

Medicine

OPEN

Numerical simulation and biomechanical analysis of locking screw caps on clavicle locking plates

Dae-Geun Kim, MD, PhD[a,*], Soo Min Kim, PhD[b], Yoonkap Kim, PhD[b]

Abstract

Background: The risk of displaced and comminuted midshaft clavicle fractures is increased in high-energy traumas such as sport injuries and traffic accidents. Open reduction and plate fixation have been widely used for midshaft clavicle fractures. Among various plates for clavicle shaft fractures, superior locking compression plates (LCPs) have been mostly used. In plate fixation, nonunion caused by implant failure is the most difficult complication. The most common reasons for metal plate failure are excessive stress and stress concentration caused by cantilever bending. These causes were easily addressed using a locking screw cap (LSC).

Methods: The clavicle 3-dimensional image was made from a computed tomography scan, and the clavicle midshaft fracture model was generated with a 10-mm interval. The fracture model was fixed with a superior LCP, and finite element analysis was conducted between the presence (*with LSC model*) and absence (*without LSC model*) of an LSC on the site of the fracture. The stresses of screw holes in models with and without LSCs were measured under 3 forces: 100 N cantilever bending force, 100 N axial compression force, and 1 N·m axial torsion force. After the finite element analysis, a validation test was conducted on the cantilever bending force known as the greatest force applied to superior locking plates.

Results: The mean greatest stress under the cantilever bending force was significantly greater than other loading forces. The highest stress site was the screw hole edge on the fracture site in both models under the cantilever bending and axial compression forces. Under the axial torsional force, the maximum stress point was the lateral first screw hole edge. The ultimate plate stress of the *with LSC model* is completely lower than that of the *without LSC model*. According to the validation test, the stiffness, ultimate load, and yield load of the *with LSC model* were higher than those of the *without LSC model*.

Conclusions: Therefore, inserting an LSC into an empty screw hole in the fracture area reduces the maximum stress on an LCP and improves biomechanical stability.

Abbreviations: CT = computerized tomography, FEA = finite element analysis, FZ = fracture zone, L = lateral, LCP = locking compression plate, LSC = locking screw cap, M = medial, MCF = midshaft clavicle fracture, 3D = 3 dimension.

Keywords: bone plate, clavicle, finite element analysis, fracture fixation, locking screw cap

1. Introduction

Midshaft clavicle fractures (MCFs) are common lesions of the scapular girdle and account for 81% of the total cases of clavicle fractures, including displaced cases (48%) and comminuted cases (19%).[1–3] Traditionally, nondisplaced and substantially displaced MCFs were managed conservatively, showing excellent results.[4] In the past, MCFs occurred in small external forces such as falls in older people, but recently, they have often been caused by high-energy traumas such as traffic accidents and sports injuries in younger people. Therefore, displaced MCFs account for approximately 48% of the total clavicle fractures, and comminuted patterns gradually increase to 19%.[3] Recently, some studies have shown a higher risk for malunion and nonunion for large displacement, which are treated nonsurgically, requiring the use of open reduction and plate fixation that show improved outcomes.[5–9]

Between an intramedullary nail and plate fixation, plate fixation (either superior or anteroinferior placement) has exhibited an excellent biomechanical strength for early exercise and provides

DGK and SMK contributed equally to this work.

This work was supported by the Soonchunhyang University Research Fund, the Technology Innovation Program (20006408) funded by the Ministry of Trade, Industry, & Energy (Korea), and the Korea Innovation Foundation (INNOPOLIS) grant funded by the Korean government, The Ministry of Science and ICT (MSIT) (2020-DD-UP-0278).

The patients provided written informed consent for the publication of clinical details and images

The authors have no conflicts of interest to disclose.

The datasets generated during and/or analyzed during the current study are available from the corresponding author on reasonable request.

The funders had no role in study design, data collection and analysis, decision to publish, or preparation of the manuscript.

[a] Department of Orthopedic Surgery, College of Medicine, Soonchunhyang University Gumi Hospital, Gumi, Republic of Korea, [b] Convergence Material Research Center, Innovative Technology Research Division, Gumi Electronics & Information Technology Research Institute (GERI), Gumi, Republic of Korea.

**Correspondence: Dae-Geun Kim, Department of Orthopedic Surgery, Soonchunhyang University Gumi Hospital, 179 1Gongda-ro, Gumi 39371, Korea (e-mail: kuroo25@schmc.ac.kr).*

How to cite this article: Kim D-G, Kim SM, Kim Y. Numerical simulation and biomechanical analysis of locking screw caps on clavicle locking plates. Medicine 2022;101:30(e29319).

Received: 2 August 2021 / Received in final form: 21 February 2022 / Accepted: 30 March 2022

http://dx.doi.org/10.1097/MD.0000000000029319

satisfactory clinical outcomes.[10,11] However, its major handicap is nonunion due to implant failure, which may require revision surgeries. The causes of plate failure are plate breakage or deformation and excessive stress concentration. Several studies suggested 2 risk factors for plate breakage: reconstruction plate usage[12] and surgical technique called bridging plate.[13,14] Moreover, a finite element analysis (FEA) on clavicle fracture plate fixation showed that the maximum stress and uneven stress concentration occur around the empty screw holes on top of the fracture area in the contoured superior reconstruction plate.[15] Another study found that the most vulnerable point of the superior clavicle locking compression plate (LCP) used for comminuted MCFs was the free screw hole above the fracture zone (FZ).[16] When lifting the arm, cantilever bending is applied, and at this time, the greatest stress is applied. Therefore, to prevent breakage, a new design consisting of superior LCPs with no screw holes on top of the FZ was proposed.[17] Nevertheless, it is virtually impossible to omit the screw holes on the fracture site during the mass production of metal plates.

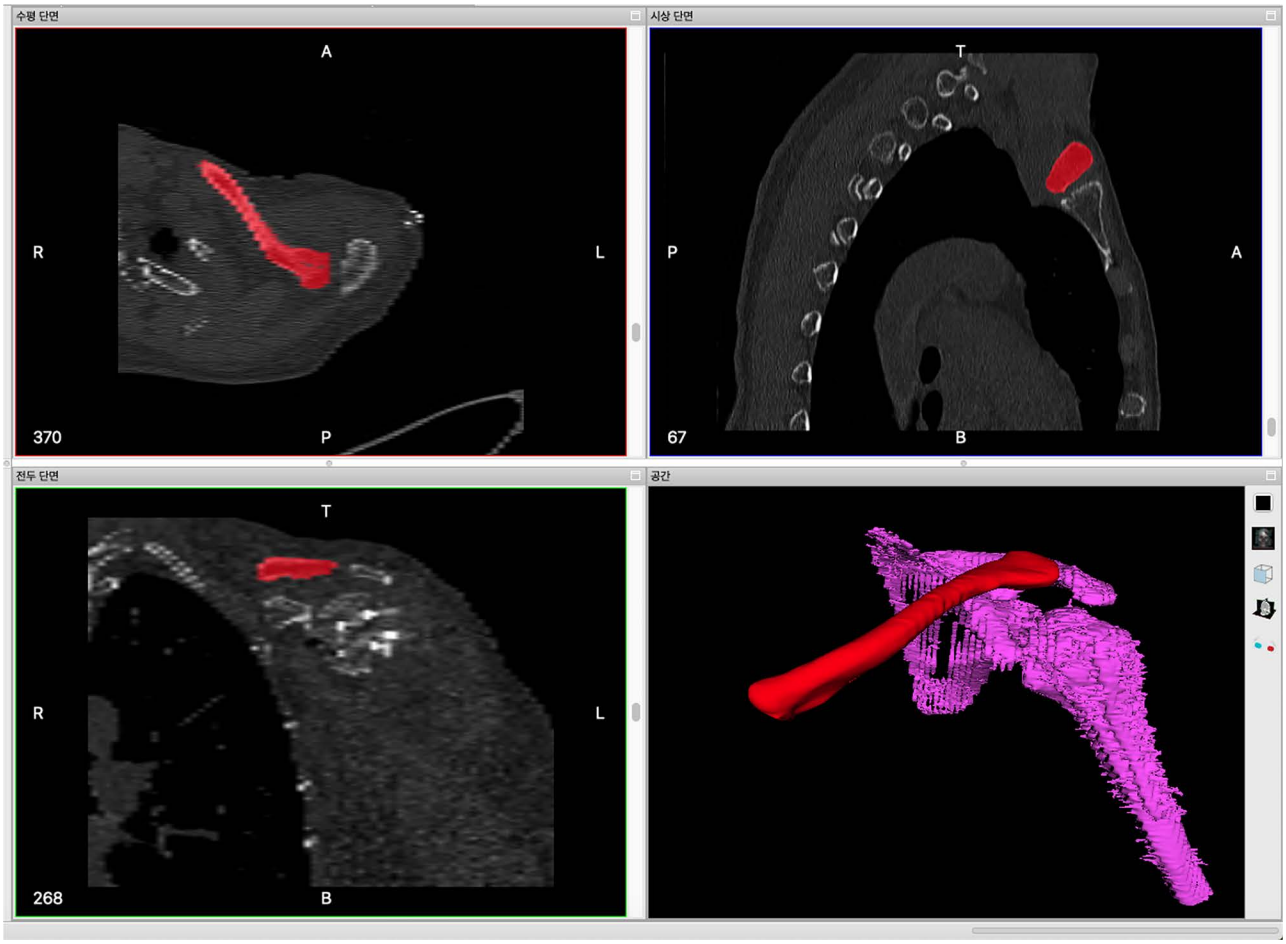

Figure 1. Conversion of axial images of clavicle CT into 3D images through the InVesalius® program. CT = computerized tomography, 3D = 3 dimension.

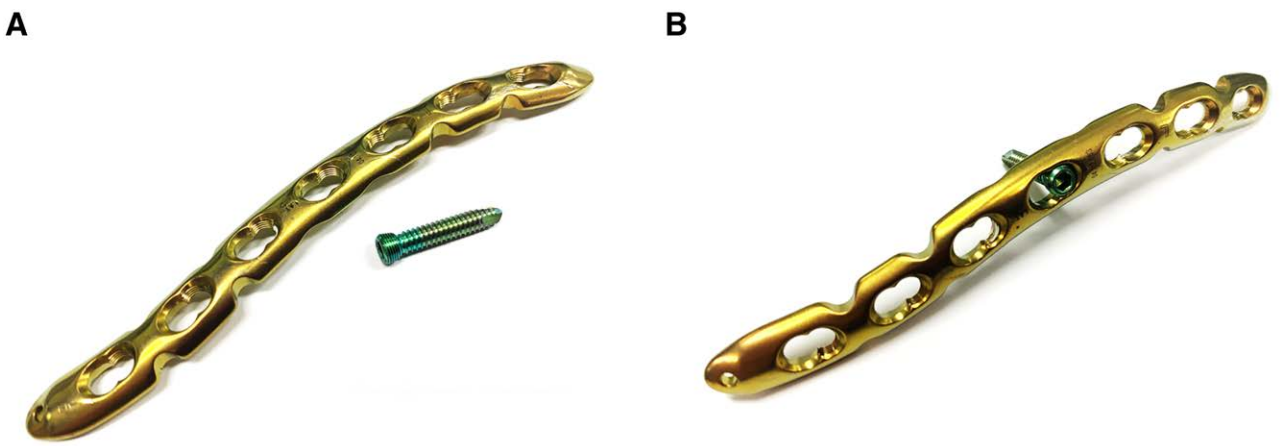

Figure 2. There was a 7-hole superior titanium alloy LCP and double thread lag screw. (A) Separated locking screw. (B) Fastened locking screw. LCP = locking compression plate.

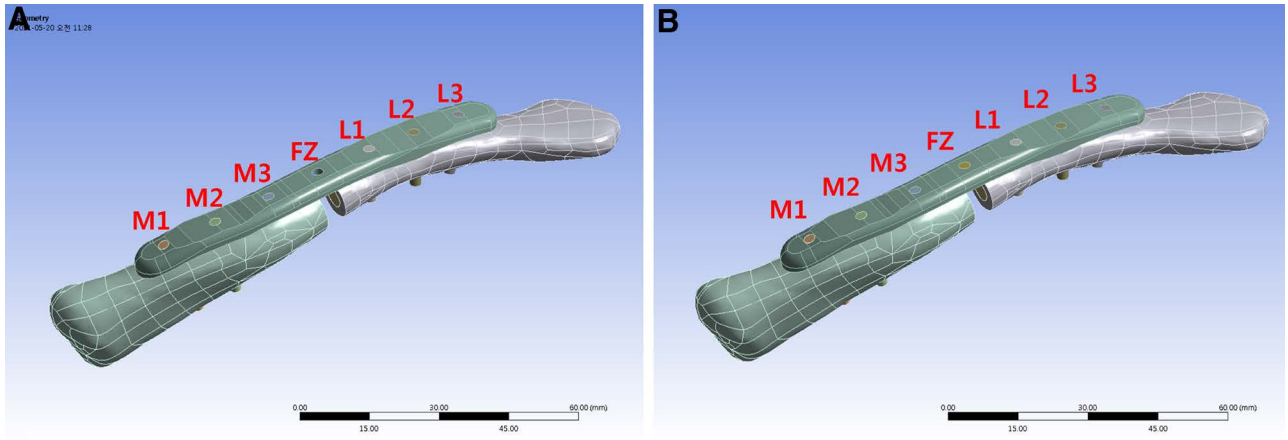

Figure 3. There were schematics of 2 simulation models. (A) Without LSC model. (B) With LSC model. LSC = locking screw cap.

Table 1

Material properties of cortical bone, cancellous bone, and titanium alloy.

Materials	Young's modulus (MPa)	Bulk modulus (MPa)	Shear modulus (MPa)
Cortical bone	17,000	14,167	6539
Cancellous bone	1000	833	385
Titanium alloy	114,000	95,000	43,846

The authors believed that a metal plate without screw holes on the fracture site and that with locking screw caps (LSCs) inserted into the screw holes in the fracture might not have the same effect, although it might be similar. We hypothesize that the plate can be strengthened by inserting LSCs into the empty screw holes on top of the FZ in displaced MCFs. We studied the stress concentration phenomenon on the empty screw hole of an LCP above the fracture position with an FEA. In addition, we theoretically verified a decentralized Von Mises stress on the LCP above the clavicle fracture using FEA.

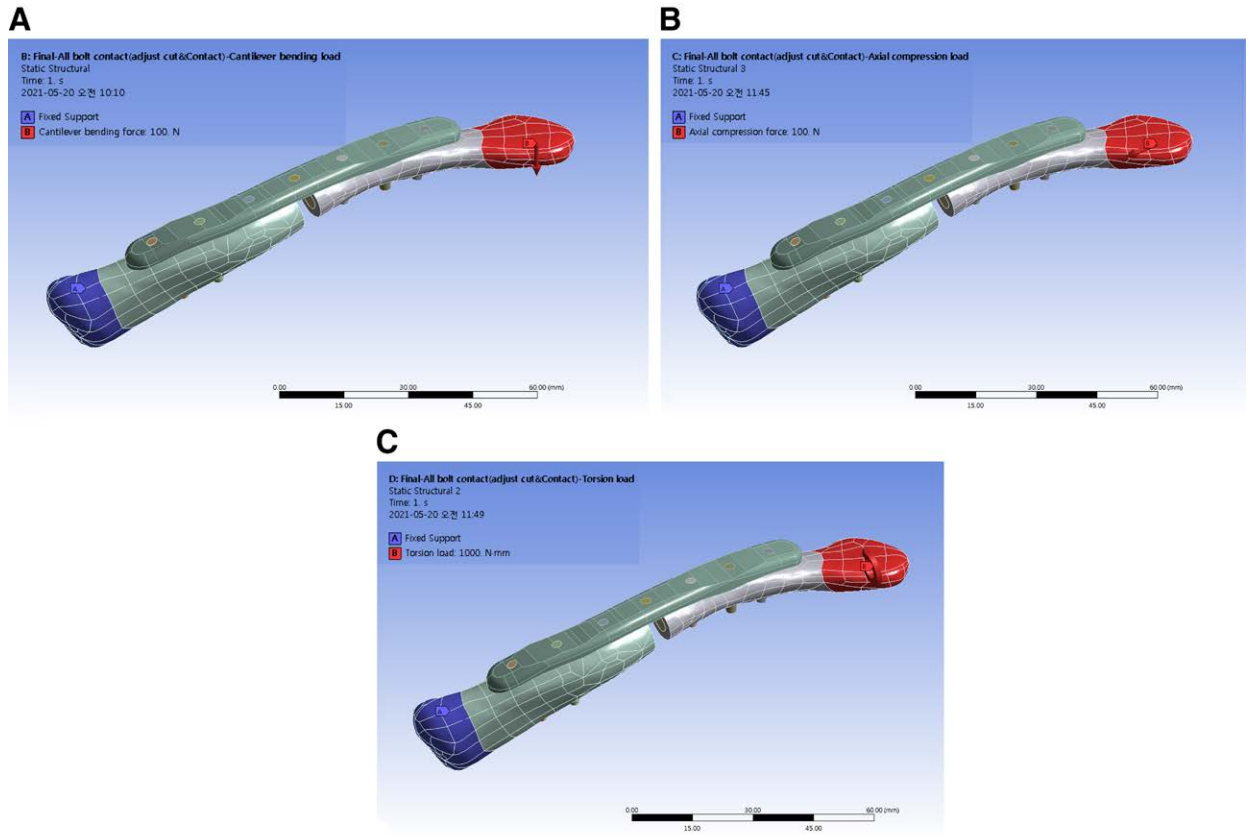

Figure 4. Three loading conditions with boundary conditions were applied to the acromial end. (A) Cantilever bending load. (B) Axial compression load. (C) Axial torsion load with count clockwise.

2. Materials and Methods

2.1. Bone modeling

The acquired images from the computerized tomography scan of the normal left clavicle to constitute the 3-dimensional (3D) clavicular model are axial images with a 1.0-mm slice thickness. These images were from a 55-year-old female volunteer, who provided written informed consent for the publication of clinical details and images. The 3D model was generated using a freeware, InVesalius (Center for Information Technology Renato Archer, Campinas, Brazil). After postprocessing, unnecessary shapes were reduced using Meshmixer (Fig. 1). We imported the 3D model into ANSYS simulation program (ANSYS, Inc., Canonsburg, PA) for FEA.

2.2. FEA model

The FE meshes were created as a tetrahedral with a 0.5-mm size for bones, screws, and plates. The orthogonal quality was 0.85907, and the average mesh element quality was 0.83861. The total elements were 1,258,688 and the mesh nodes were 1,843,793. There was a 10-mm fracture interval between the medial and lateral fragments, indicating the presence of a comminuted MCF.

Table 2

Stress analysis results by FEA.

	Cantilever bending load (MPa)		Axial compression load (MPa)		Axial torsion load (MPa)	
Points	**Without LSC**	**With LSC**	**Without LSC**	**With LSC**	**Without LSC**	**With LSC**
M1	15.40	15.54	0.78	0.78	3.60	3.81
M2	36.71	36.28	5.32	5.34	10.10	10.60
M3	91.01	90.17	21.91	21.94	24.43	24.95
FZ	874.11	412.66	244.51	116.88	46.90	61.03
L1	82.13	80.01	24.99	24.33	33.47	33.57
L2	39.88	40.22	11.50	11.56	24.71	25.34
L3	16.17	15.79	3.99	3.82	5.20	4.43
Avg. M	47.71	47.33	9.34	9.35	12.71	13.12
Avg. L	46.06	45.34	13.49	13.23	21.13	21.11
Avg. ratio (M/L)	1.04	1.04	0.69	0.71	0.60	0.62
Max	874.11	494.26	252.22	114.15	86.03	83.23
FZ reduce (%)	52.79		52.20		–30.11	
Max reduce (%)	43.46		54.74		3.25	

Avg. = average, FZ = fracture zone, L = lateral, LSC = locking screw cap, M = medial.

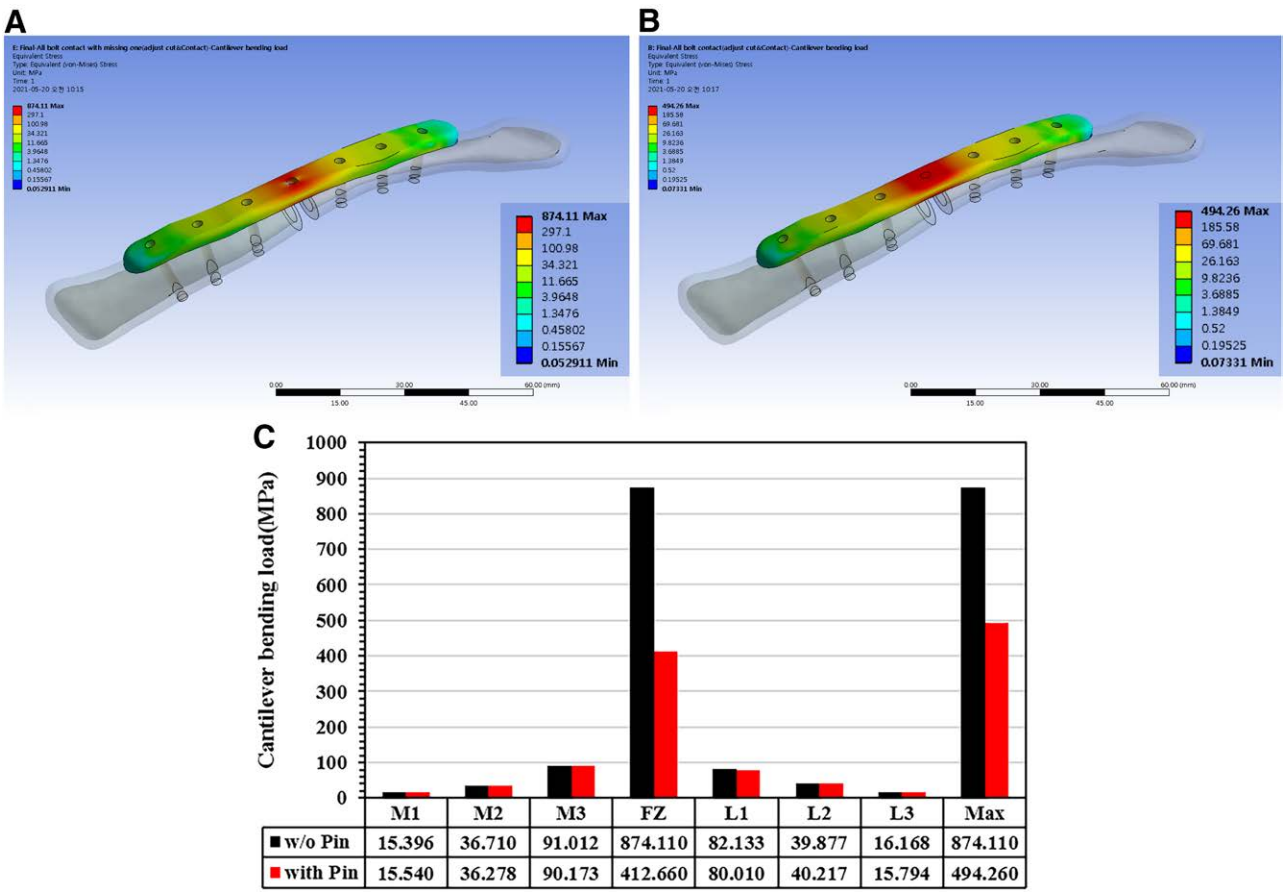

Figure 5. FEA simulation showed Von Mises stress distribution of the LCP under cantilever bending force. Stress concentration was evenly distributed in with LSC model. (A) Without LSC model. (B) With LSC model. LCP = locking compression plate, LSC = locking screw cap.

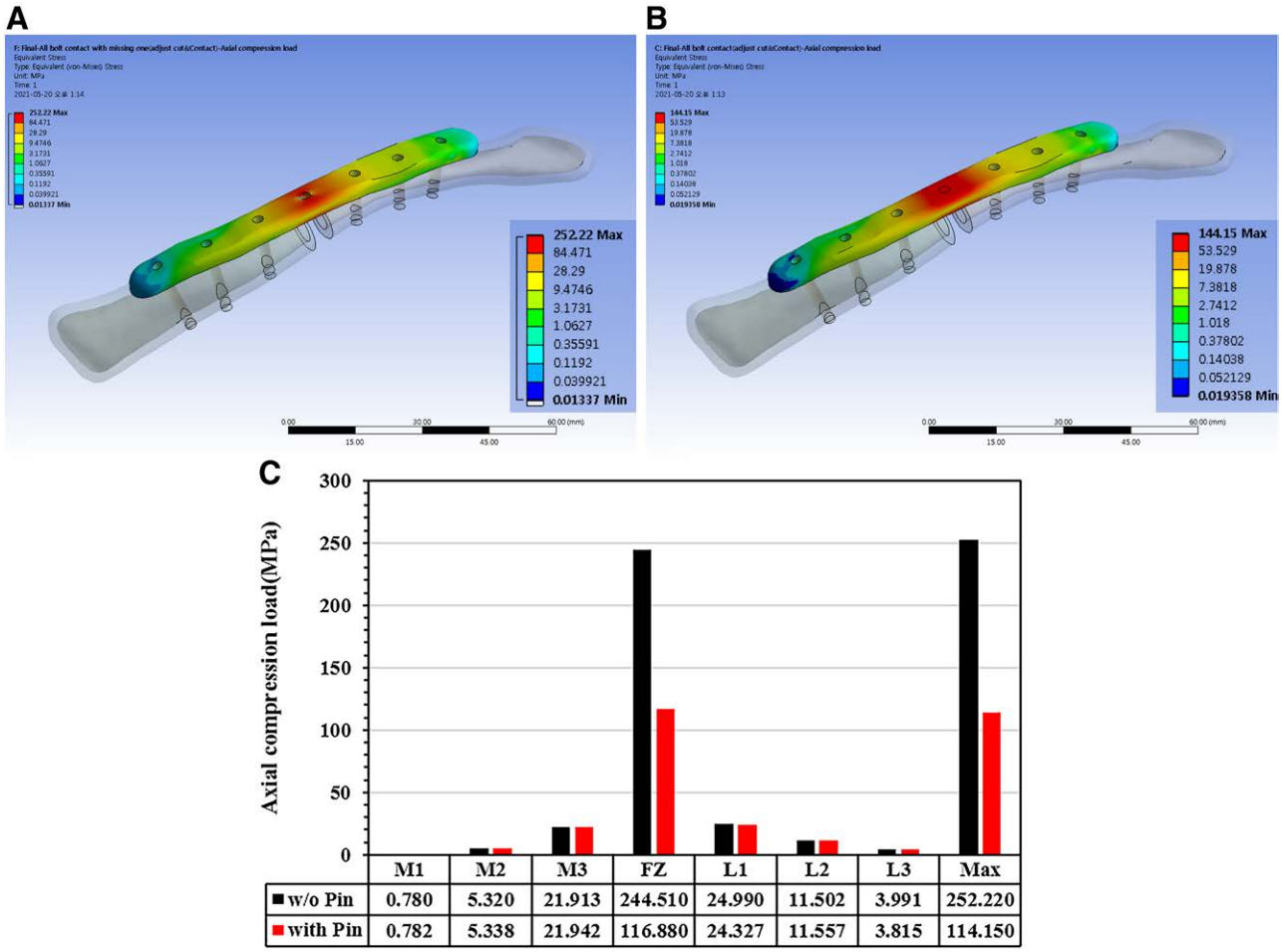

	M1	M2	M3	FZ	L1	L2	L3	Max
w/o Pin	0.780	5.320	21.913	244.510	24.990	11.502	3.991	252.220
with Pin	0.782	5.338	21.942	116.880	24.327	11.557	3.815	114.150

Figure 6. There was an FEA simulation of Von Mises stress distribution under axial compression conditions. Also, stress concentration was evenly distributed in with LSC model. (A) Without LSC model. (B) With LSC model. FEA = finite element analysis, LSC = locking screw cap.

This fracture model was secured with a 2.5-mm 7-hole superior titanium alloy LCP and modeled using an LCP superior clavicle plate (AO Synthes, Solothurn, Switzerland; Fig. 2). To simplify the simulation, the combi-holes were replaced by single locking holes. Two models were used in this study: the fracture model, which was secured with 6 locking screws on the medial and lateral sides without an LSC (*without LSC model*), and the other model presents the design in which an LSC was inserted into an empty screw hole above the fracture (*with LSC model*; Fig. 3).

2.3. Boundary condition and loads

According to the property of the locking plate, the screw is strongly combined with the plate owing to the screw tension between the screw and LCP as shown in Figure 2. In addition, the screws penetrate the cortical bone and are then combined with it by the screw tension. This study aims to determine whether the magnitude of stress transmitted to the LCP because of the generated external force can be relieved in the patient's daily activities. Therefore, we studied the dispersion characteristics of the stress concentration in the LCP with the external force under a condition that does not cause additional crushing of the clavicle because of the screw tension. In the case of the application of the screw structure with the LCP, the geometrical complexity is greatly increased, and the structural variable with the screw thread can also affect the observation of the stress distribution at the fracture area. Therefore, we simply defined the screw coupling area in the form of a column. In addition, the pattern of the stress distribution was analyzed by defining the screw and the clavicle to be in complete contact because it is assumed that the range in which the crushing of the clavicle does not occur. The contact interface between the bone–plate, plate–screws, and bone–screws was set as a fully bonded condition. The material properties of the cortical bone, cancellous bone, and titanium alloy were applied per the references (Table 1).[16,18] The types of fractures that occurred in the clinical setting and the shape of the clavicle were different. To proceed with simulations for the different types of fractures, we applied the cortical alignment fracture type with the simplest geometric structure in this study.[2]

As in the previous studies, 3 loading modes were applied at the acromial end: 100 N for the cantilever bending, 100 N for the axial compression, and 1 N·m for anticlockwise axial torsion for the case of the raised arm (Fig. 4).[15–17,19]

The distribution of stress in the plate was measured using simulation. The stresses on 7 points representing the 7 locking holes of the superior LCP, that is, the medial (M) M1, M2, and M3; FZ; lateral (L) L1, L2, and L3 and ultimate stress of both models for all 3 forces were analyzed as the Von Mises stress (Fig. 3).

2.4. Validation test

To validate the results, the confirmation was performed under the cantilever bending force, which was the greatest difference in the maximal plate stress between model A and model B. To measure mechanical properties, metal plates were inserted into a prepared

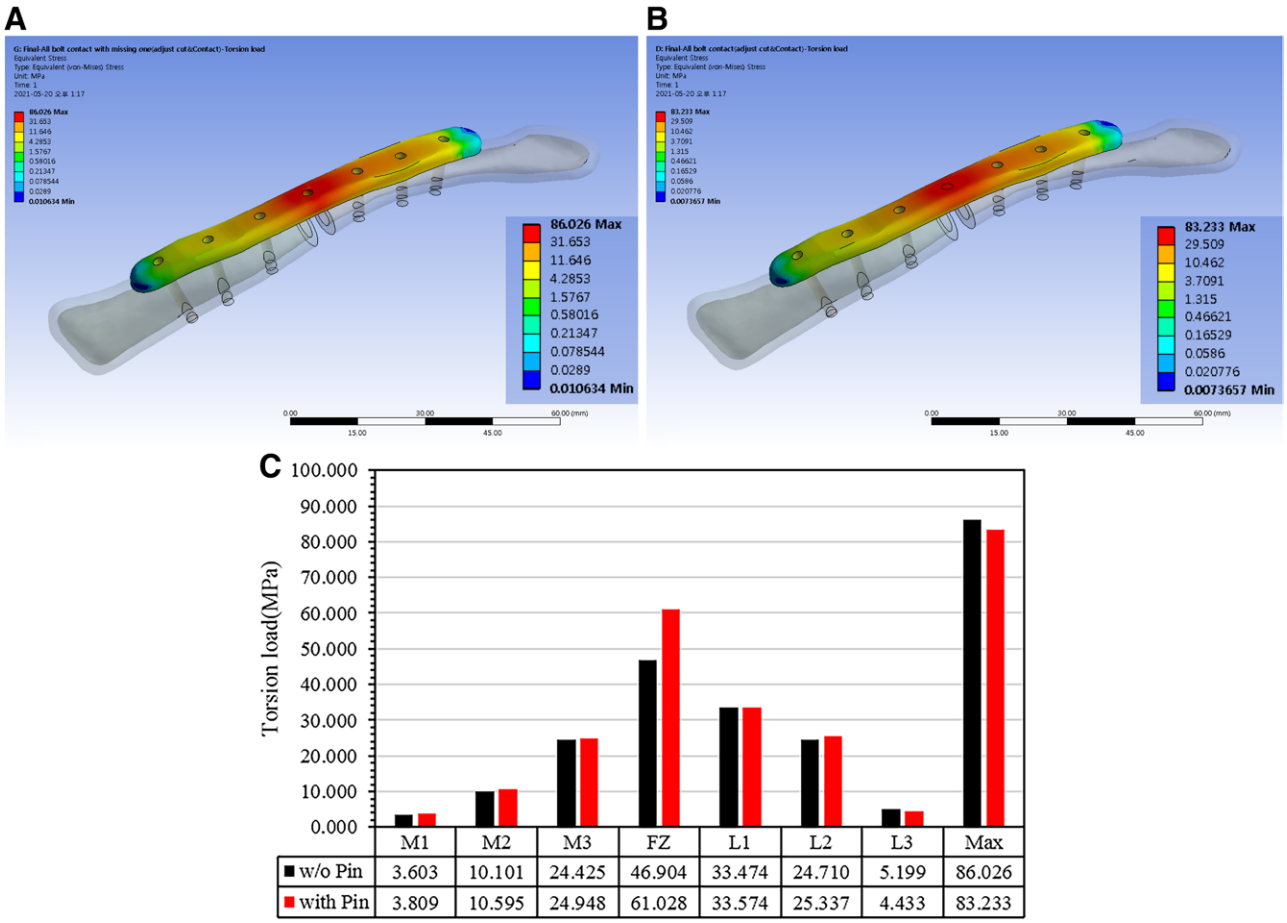

	M1	M2	M3	FZ	L1	L2	L3	Max
w/o Pin	3.603	10.101	24.425	46.904	33.474	24.710	5.199	86.026
with Pin	3.809	10.595	24.948	61.028	33.574	25.337	4.433	83.233

Figure 7. Clavicle LCP FEA simulation showed Von Mises stress distribution under axial torsion loading. The stress distribution was similar, but the magnitude was shown to be smaller in with LSC model. (A) Without LSC model. (B) With LSC model. FEA = finite element analysis, LCP = locking compression plate, LSC = locking screw cap.

jig, and a force was applied at a maximum speed of 10 mm/min. The stiffness, field load, and ultimate load were obtained.

3. Result

3.1. FEA result

The Von Mises stresses for both models are listed in Table 2. In the cantilever bending force, the stress of M1, M2, M3, L1, L2, and L3 in both models are alike with an average ratio (M/L) of 1.04. However, the stress of the FZ was significantly reduced after inserting an LSC, from 874.11 MPa in the *without LSC model* to 412.66 MPa in the *with LSC model*. This means that the cantilever bending force applied to the fracture model is not concentrated entirely on the LCP combined with the clavicle but mostly on the FZ point. In addition, it shows that the stress is uniformly concentrated on both sides of the fracture area.

The maximum stress point in the *without LSC model* was the FZ point, and the maximum stress of the *without LSC model* (874.11 MPa) was larger than that of the *with LSC model* (494.26 MPa) under the cantilever bending force (Fig. 5). Similar trends were observed under the axial compression loading. Under axial compression loads, the stress of the FZ was significantly reduced from 244.51 MPa in the *without LSC model* to 116.88 MPa in the *with LSC model* (Fig. 6), and the maximum stress of the *without LSC model* (252.22 MPa) was larger than that of the *with LSC model* (114.15 MPa; Table 2).

However, for the FZ stress, this relationship was not observed in the anticlockwise torsion force (Fig. 7). The highest stress of the *with LSC model* (83.23 MPa) was slightly lesser than that of the *without LSC model* (86.03 MPa) although the Von Mises stress of the FZ point increased even when an LSC was inserted (*without LSC model*: 46.90 MPa and *with LSC model*: 61.03 MPa).

3.2. Validation result

The average stiffness of the *without LSC model* is 18.05 N/mm, which is 1.47 N/mm lower than that of the *with LSC model* of 19.52 N/mm (Table 3). The yield load, which is the load elastic deformation change to plastic deformation, was 111.81 N for the *without LSC model* and 128.03 N for the *with LSC model*. The ultimate load, which is the load at the time of destruction, was 122.28 N in the *without LSC model* and 141.00 N in the *with LSC model* improving the mechanical properties of the metal plate against cantilever bending. The result of the validation test confirms the FEA result and our hypothesis.

4. Discussion

Managing displaced MCFs remains a challenge. A meta-analysis study recently revealed that surgery for displaced MCFs increases the possibility of union after 12 months of follow-up.[9] More than 10% of patients who are reluctant to undergo surgery for acute displaced MCFs may be more likely to encounter nonunion. Therefore, undergoing surgery for acute displaced fractures is recommended to lower the chance of nonunion and malunion.[19]

Table 3

The result of validation test.

Specimens	Stiffness (N/mm)	Yield load (N)	Ultimate load (N)
Without LSC model			
1	18.03	112.96	123.14
2	18.08	111.56	123.87
3	18.05	110.92	119.83
Avg	18.05	111.81	122.28
SD	0.02	1.04	2.15
With LSC model			
1	19.84	131.59	142.45
2	19.26	123.57	139.37
3	19.46	128.94	141.18
Avg	19.52	128.03	141.00
SD	0.30	4.09	1.55

LSC = locking screw cap, SD = standard deviation.

Plate fixation has been the gold-standard treatment for displaced MCFs. Between the plate and intramedullar nail, plate fixation biomechanically provides a more stable strength for an early range-of-motion exercise. However, implant failure is one of its limiting factors. A risk factor for plate breakage or bending was the increased stress in the free hole around the FZ. Therefore, some finite element studies recommend different types of plates, such as anterior plates, spiral plates, and superior plates with no screw holes above the fracture area.[17,18,20,21]

A comminuted MCF model was secured with a 7-hole titanium superior LCP, and FEA was performed between the *with LSC model* and without LSC model on top of the fracture site. The 7 stress measurement points represent the stress geometrically generated at the same point on the edge of the LCP hole. Hence, the measurement point and the maximum stress concentration point of the LCP could be different, and the magnitude of the stress generated at the same location was analyzed to determine the effectiveness of this model. In addition, the magnitude of the maximum stress applied to the entire LCP was separately indicated to analyze the variation of the magnitude of the concentrated maximum stress. In the case of the cantilever bending load, the values of the FZ point and the maximum stress point are the same in the *without LSC model*. This means that the maximum stress concentration point is the same as the FZ point. However, the values of the FZ point and the maximum stress point of the *with LSC model* are 412.66 and 494.26 MPa, respectively. It indicates that the locations of the maximum stress concentration point and the FZ point are different in the *with LSC model*.

The FZ stress of the *without LSC model* from the cantilever bending force (874.110 MPa) was much higher than the maximal stress from the axial compression (244.510 MPa) and the axial torsion force (46.904 MPa; Table 2). This means that the cantilever loading force is the biggest load on an implant and can be the main cause of implant failure.

Compared to the *without LSC model*, the *with LSC model* reduced the stress on the FZ point by 52.8% in the cantilever bending force and 52.2% in the axial compression force.

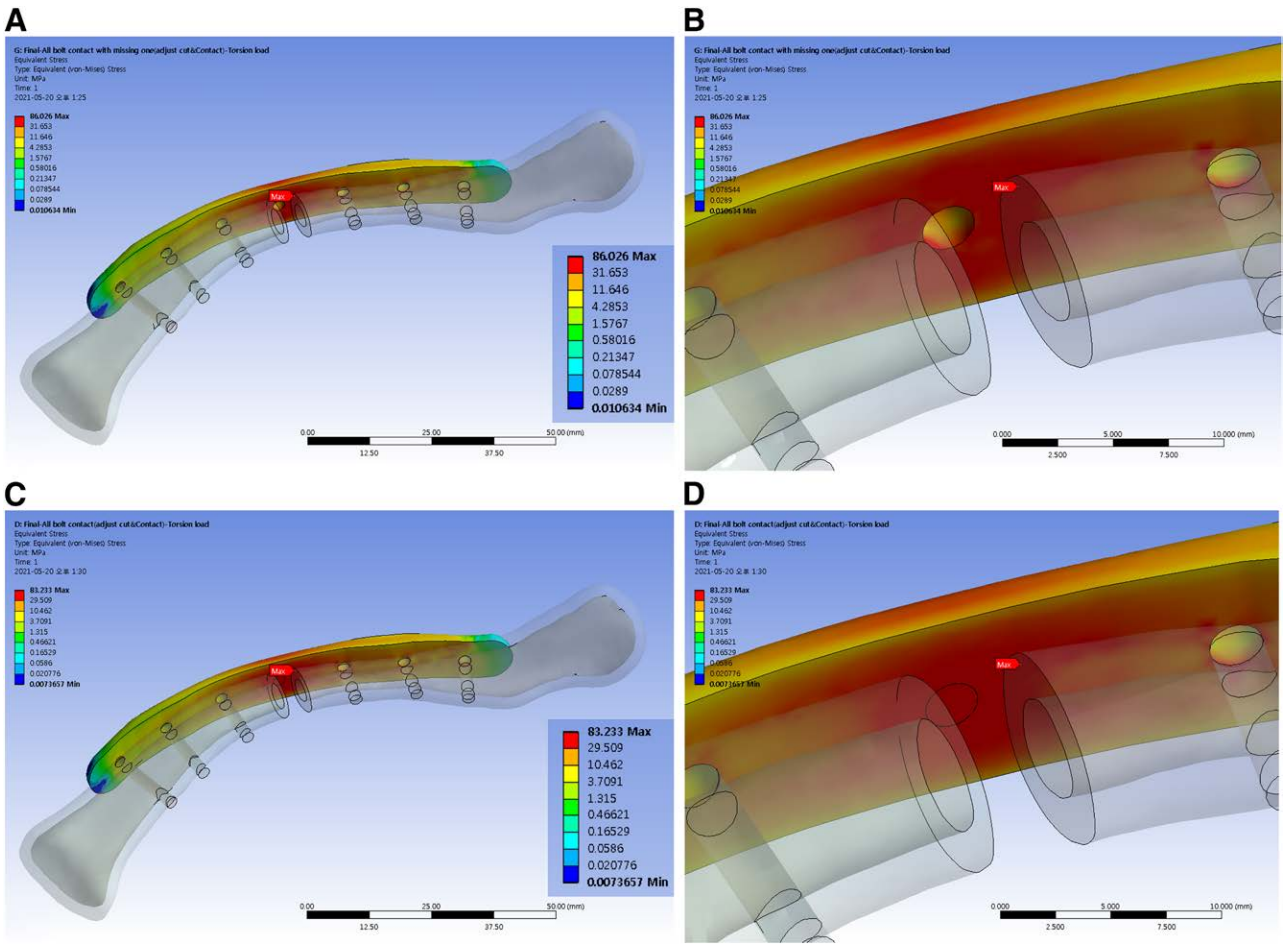

Figure 8. Under the axial torsional load, the maximum stress point was not the FZ point like the other 2 conditions. The peak stress point moved to the L1 point of the rear side plate in both models. (A) Without LSC model. (B) Enlarge without LSC model. (C) With LSC model. (D) Enlarge with LSC model. FZ = fracture zone, LSC = locking screw cap.

However, the highest stress on the FZ point in the *with LSC model* (61.03 MPa) was approximately 1.3 times higher than that in the *without LSC model* (46.90 MPa) in the counterclockwise torsion force. Nonetheless, the maximal stress of the LCP was low in the *with LSC model* under the 3 loading conditions, and the most important difference was observed in the cantilever bending force.

In addition, no significant difference occurred between the FZ point and the maximum stress point under the cantilever bending and axial compression loads. However, unlike the situations under the other stress conditions, in torsion, the maximum stress point moved to another position (Fig. 8). At the FZ point, the stress level increased by 30.11%, showing poor results, but the absolute value of the stress was twice as low as the other 2 stress conditions. This indicates that the result with torsion could not significantly affect the structural properties of the LCP. In addition, the maximum stress concentration point shifted, but its value decreased by 3.25%. The maximum stress point was changed because the counterclockwise moment moved the force vector in a different direction. It can be inferred that the peak stress point moved to the L1 direction of the rear side plate, showing the same result for both models. Therefore, it could be analyzed as an increase in stiffness, considering the overall structural characteristics of the LCP.

As reported in previous studies, the screw hole above the FZ was confirmed to be a delicate point in the superior clavicle LCP, particularly in terms of the cantilever bending force. The *with LSC model* showed better biomechanical properties than the *without LSC model* in all the loads. Therefore, we can easily lower the maximal stress and make the stress concentration uniform by inserting LSCs into the free screw holes around the FZ. There are some limitations to this study. First, the fracture is complex and very complicated in the real world, and the actual number of fracture cases varies widely. Second, there are several considerations that could not be embodied in simulation. Some of the implementable difficulties include changes in clavicle anatomy, micromotion between bones and plates, stress-raising effects of screws, and bone quality. To simplify the simulation, these considerations were excluded. Third, the strength of the applied forces was not reflected in the magnitude of the force acting on the body but rather as a relative characteristic of the force direction. Further studies will require analysis of various bone anatomy and fracture patterns. Moreover, studies on the screw size, number, and location should also be conducted.

In conclusion, inserting the LSCs relieves the stress concentration, confirming that the stress concentrated at the FZ point in the same distribution condition is rapidly reduced. Hence, the biomechanical stability of the superior LCP could be easily improved by inserting LSCs into the empty screw holes in the fracture area.

Author contributions

Conceptualization, study design: Dae-Geun Kim.
Data curation: Soo Min Kim.
Investigation & methodology: Dae-Geun, Soo Min Kim.
Software & visualization: Soo Min Kim.
Validation: Dae-Geun Kim
Writing – original draft: Dae-Geun Kim.
Writing – review & editing: Yoonkap Kim.

References

[1] Nordqvist A, Petersson C. The incidence of fractures of the clavicle. Clin Orthop Relat Res. 1994;300:127–32.
[2] Robinson CM. Fractures of the clavicle in the adult. Epidemiology and classification. J Bone Joint Surg Br. 1998;80:476–84.
[3] Postacchini F, Gumina S, De Santis P, et al. Epidemiology of clavicle fractures. J Shoulder Elbow Surg. 2002;11:452–6.
[4] Rowe CR. An atlas of anatomy and treatment of midclavicular fractures. Clin Orthop Relat Res. 1968;58:29–42.
[5] Lazarides S, Zafiropoulos G. Conservative treatment of fractures at the middle third of the clavicle: the relevance of shortening and clinical outcome. J Shoulder Elbow Surg. 2006;15:191–4.
[6] van der Meijden OA, Gaskill TR, Millett PJ. Treatment of clavicle fractures: current concepts review. J Shoulder Elbow Surg. 2012;21:423–9.
[7] Axelrod DE, Ekhtiari S, Bozzo A, et al. What is the best evidence for management of displaced midshaft clavicle fractures? A systematic review and network meta-analysis of 22 randomized controlled trials. Clin Orthop Relat Res. 2020;478:392–402.
[8] Jia Z, Li W, Qin Y, et al. Operative versus non-operative treatment in complex proximal humeral fractures: a meta-analysis of randomized controlled trials. Orthopedics. 2014;37:e543–51.
[9] Zlowodzki M, Zelle BA, Cole PA, et al. Evidence-Based Orthopaedic Trauma Working Group. Treatment of acute midshaft clavicle fractures: systematic review of 2144 fractures: on behalf of the evidence-based orthopaedic trauma working group. J Orthop Trauma. 2005;19:504–7.
[10] Nourian A, Dhaliwal S, Vangala S, et al. Midshaft fractures of the clavicle: a meta-analysis comparing surgical fixation using anteroinferior plating versus superior plating. J Orthop Trauma. 2017;31:461–7.
[11] Woltz S, Krijnen P, Schipper IB. Plate fixation versus nonoperative treatment for displaced midshaft clavicular fractures: a meta-analysis of randomized controlled trials. J Bone Joint Surg Am. 2017;99:1051–7.
[12] Chiu YC, Huang KC, Shih CM, et al. Comparison of implant failure rates of different plates for midshaft clavicular fractures based on fracture classifications. J Orthop Surg Res. 2019;14:220.
[13] Iannotti MR, Crosby LA, Stafford P, et al. Effects of plate location and selection on the stability of midshaft clavicle osteotomies: a biomechanical study. J Shoulder Elbow Surg. 2002;11:457–62.
[14] Meeuwis MA, Pull Ter Gunne AF, Verhofstad MH, et al. Construct failure after open reduction and plate fixation of displaced midshaft clavicular fractures. Injury. 2017;48:715–9.
[15] Marie C. Strength analysis of clavicle fracture fixation devices and fixation techniques using finite element analysis with musculoskeletal force input. Med Biol Eng Comput. 2015;53:759–69.
[16] Huang X, Xiao H, Xue F. Clavicle nonunion and plate breakage after locking compression plate fixation of displaced midshaft clavicular fractures. Exp Ther Med. 2020;19:308–12.
[17] Pengrung N, Lakdee N, Puncreobutr C, et al. Finite element analysis comparison between superior clavicle locking plate with and without screw holes above fracture zone in midshaft clavicular fracture. BMC Musculoskelet Disord. 2019;20:465.
[18] Huang TL, Chen WC, Lin KJ, et al. Conceptual finite element study for comparison among superior, anterior, and spiral clavicle plate fixations for midshaft clavicle fracture. Med Eng Phys. 2016;38:1070–5.
[19] Vannabouathong C, Chiu J, Patel R, et al. An evaluation of treatment options for medial, midshaft, and distal clavicle fractures: a systematic review and meta-analysis. JSES Int. 2020;4:256–71.
[20] Zhang F, Chen F, Qi Y, et al. Finite element analysis of dual small plate fixation and single plate fixation for treatment of midshaft clavicle fractures. J Orthop Surg Res. 2020;15:1–7.
[21] Zhang X, Cheng X, Yin B, et al. Finite element analysis of spiral plate and Herbert screw fixation for treatment of midshaft clavicle fractures. Medicine (Baltimore). 2019;98:e16898.